

## SPAR VIM MODEL TESTS AT SUPERCRITICAL REYNOLDS NUMBERS

**Tim Finnigan**  
Chevron Energy Technology Company

**Dominique Roddier**  
Marine Innovation & Technology

### ABSTRACT

There have been a number of publications on spar Vortex-Induced-Motions (VIM) model testing procedures and results over the past few years. All tests allowing full 6 DOF response to date have been done under sub-critical Reynolds Number conditions. Tests under super-Critical Reynolds Number conditions have only been done with a fully submerged 1 DOF rig. Early in 2006, Chevron Energy Technology Company (CETC) completed a series of model tests to investigate the effect of Reynolds Number and hull appurtenances on spar vortex induced motions (VIM) for a vertically moored 6DOF truss spar hull model with strakes. Tests were done at both sub and super-critical Reynolds Numbers, with matching Froude Numbers. In order to assess the importance of appurtenances (chains, pipes and anodes) and current heading on strake effectiveness, tests were done with several sets of appurtenances, and at various headings and reduced velocities.

This paper addresses the challenges of performing spar VIM model tests at Super Critical Reynolds Numbers, and how they were resolved without the restrictions noted in earlier publications. Certain aspects of the effect of appurtenances and current heading on strake effectiveness and VIM response are discussed.

### BACKGROUND

Spar platforms in their various forms – classic, truss, cell – have been adopted by the offshore industry for deep and ultra-deepwater oil and gas production because they are resistant to heave motions in waves. However, their shape makes them susceptible to Vortex-Induced-Motions, or VIM.

Transverse VIM occurs when the vortices which are formed as the flow moves past the spar are shed alternatively on each side of the hull at a frequency close to the natural frequency of the moored system.

Early in the development of the spar concept, it was believed that a spar platform would not undergo VIM because the aspect ratio (length divided by diameter) was too small, with “classic” spars conceived with a hull diameter of about 100 ft. and a draft of about 600 ft. Vortex-Induced-Motions, or more commonly referred to as Vortex-Induced-Vibrations (VIV) for long slender structural members such as cables and risers, was thought to be possible only for very long, slender objects.

Model tests soon proved that hypothesis wrong. But the spar concept held tremendous promise for the offshore industry by virtue of their ability to resist wave-induced motions. So various strake configurations were conceived and tested. One of the major spar contractors finally settled on a 3 start helical strake design with 10% strake heights (strake height divided by hull diameter) and 5:1 pitch (the height to diameter ratio for one wrap of the strake).

There was concern even back then that scale effects might be important, so rudimentary yet expensive tests were performed to determine if strakes were still effective at flow conditions considered to be more typical of proto-type spar platforms [1]. Those tests seemed to confirm the findings from the smaller scale tests that 3-start 10% high 5:1 pitch strakes mitigated VIM. Hence, the early “classic” spars were designed with the confidence gained from these rudimentary model tests.

However, all three of those spars experienced VIM amplitudes that exceeded the limits established in those early model tests [1]. That led to a flurry of further model testing and changes in model test procedures to understand why those previous tests failed to accurately predict field behavior. One of the key findings from those tests was that geometry had a large effect (“test what you build, and build what you test”). Yet debate still remained as to whether scale effects are important.

Reynolds Number scaling and Froude Number scaling are the two relevant scaling parameters for hydrodynamic model testing of offshore structures [2, Chapter 9]

The Reynolds Number,  $R_e$ , is defined as

$$R_e = \frac{VD}{\nu} \quad (1)$$

where  $V$  is the flow velocity,  $D$  is the hull diameter, and  $\nu$  is the kinematic viscosity of the fluid.

The Froude Number,  $F_r$ , is defined as

$$F_r = \frac{V}{\sqrt{gD}} \quad (2)$$

where  $g$  is the gravitational constant.

However, satisfying both the Reynolds and Froude scaling simultaneously for spar model scale tests is not practical. Care must be taken to avoid high Froude Numbers (e.g., greater than approximately 0.25), which could induce large bow waves that increase damping and decrease VIM response. So in order to match the Reynolds Number as well, either the gravity would need to be significantly increased, or the viscosity of the testing fluid significantly decreased.

It is believed by some that it is important to test at supercritical Reynolds Numbers in order to attain a flow regime which is similar to the flow experienced in full scale [3, 4]. However, up until these present tests, only 1-DOF spar models have been tested in supercritical flow conditions.

A contrasting hypothesis is that for a helically straked cylinder, flow separation is controlled by the sharp edges of the strakes and not by boundary layer effects [5]. That means that smaller scale tests should be sufficient to quantify the VIM behavior, provided the geometry is accurately modeled.

Further, some spar model tests have shown the importance of including other modes of oscillation (e.g. surge, sway, heave, roll, pitch, and yaw), as the spar might lock-in to sway at lower velocities and roll at higher velocities [6]. The two degrees of freedom could actually couple (lock-in simultaneously). In this case it is important that the sway and roll modes and periods be properly scaled.

Up until the present tests, the only way to assess the potential for lock-in by other modes or coupled modes was to test a vertically moored 6-DOF model at sub-critical Reynolds Numbers.

Neither testing method (super-critical, submerged, 1-DOF tests or sub-critical, freely floating, 6-DOF tests) appeared to satisfy all concerns. It was believed to be not possible or not practical to test a freely floating spar model in 6-DOF and under super-critical flow conditions.

Last year, Chevron completed a model test program which satisfied both the 6-DOF motion requirements and the super-critical flow regime, while maintaining proper Froude Number scaling to eliminate concerns over free surface effects on the VIM behavior. To complement those tests and fully assess the importance of Reynolds Number, identical model test programs were completed at two smaller scales. However, presentation of those comparison results is beyond the scope of this paper.

## MODEL TEST BASIS

The following are important parameters in VIM model testing:

- Geometric scaling (Diameter, draft, appurtenances)
- Dynamic scaling (GM, period ratios, mass ratio)
- Hydrodynamic scaling ( $R_e$ ,  $F_r$ )
- Mooring stiffness
- Degrees of freedom
- Current direction and profile
- Directional resolution
- Damping introduced by the test rig
- Blockage (wall) effects
- Record length (number of response cycles)

The four largest towing basins in the world were evaluated for the present model tests. None of the model basins were deep enough to test a classic spar at super-critical Reynolds Numbers. However, they were all deep enough to test a truss spar hull. The David Taylor Model Basin (DTMB) in Bethesda, Maryland was chosen for the tests, and a generic truss spar hull was selected as the model. Earlier tests had demonstrated that models with small aspect ratio would still undergo significant VIM [7]. Further, by excluding the truss in the tests, any questions about the scalability of the small diameter truss members would be eliminated.

Additional test features are:

- Hull appurtenances (chains, external pipes, mooring system, strakes and anodes) are modeled.
- Tests are done with and without these appurtenances
- The model is tested at multiple and closely spaced headings.

## Dynamic Similitude

Dynamic scaling is associated with the vessel's rigid body modes, mass ratio, and reduced velocity,  $V_{rn}$ . The reduced velocity is an important non-dimensional parameter in VIM which relates the flow velocity and the natural period and hull diameter.

$$V_{rn} = VT_n/D$$

where,

- $V$  = the characteristic current velocity, typically the highest velocity in the current profile
- $T_n$  = the still water natural period of the moored vessel transverse to the current direction under mean load

It is often important to include all modes of oscillation (e.g. surge, sway, heave, roll, pitch, and yaw) since the spar might lock-in to sway at lower velocities and roll at higher velocities [6]. The two degrees of freedom might actually couple (lock-in simultaneously). In this case it is important that the sway and roll modes and periods be properly scaled.

### Geometric Similitude

Geometric similitude is achieved when the geometry of the model and prototype bodies is similar. The geometry of the hull and strakes (if appropriate) should be accurately scaled. This includes any construction openings in the strakes, brackets (which might affect the flow along the strakes), chains, anodes, external pipes and other appurtenances that may affect the flow around the body.

Some members, e.g. the truss members of a truss spar, may result in viscous damping effects that are Reynolds Number dependent. In order to avoid the uncertainties modeling of these members would have on the results, they have been left out. Therefore, the VIM quantities measured in these tests are considered to be somewhat conservative for a truss spar.

### Mooring Stiffness

In these tests, a linear symmetric mooring system is used for the model test set-up. The reduced velocity ( $V_m$ ) is used as a design parameter. In this case, the VIM response in the model is related to the design A/D via the reduced velocity. In the model tests, the spar response is measured at different reduced velocities. In order to apply the results in design, the transverse period of the spar is calculated at different offsets, from which  $V_m$  is determined. Then for each offset, the A/D as a function of  $V_m$  is determined.

### Damping

Damping can affect VIM response, therefore the damping (hydrodynamic and mechanical) generated in the model basin should be consistent with the damping expected in the field. Since mechanical damping may be generated by the testing equipment and is absent in the field, care needs to be taken to understand the effect of damping on the VIM response and to mitigate such effects [4]. Hydrodynamic damping due to mooring lines and wave effects are considered in the model test design set-up.

### Length of Response Record

Sufficiently long response time histories are required to provide meaningful statistics such as standard deviation, significant, and maximum values. When the vortex-induced motion is well developed and sustained (e.g., fully locked-in),

relatively few cycles are required to establish the maximum VIM amplitude. If the VIM response is modulated (e.g., in the lock-in and lock-out transition regions), long records are required to establish statistical values. It is shown in previous VIM tests that multiple repeat runs produce similar extremal statistics as long records [7]. Since very long records are not possible in these tests, repeats are run to verify the statistics.

### Tow speeds and headings selected

Vortex-Induced-Motions are negligible when  $V_{rn}$  is below a threshold value of approximately 4. Further, beyond a range of  $V_{rn}$  from 7 to 9, the motion starts to lock-out. In these tests, it is impractical to test beyond a  $V_{rn}$  of 10 due to loads in the mooring load cells and basin length. Therefore tests are conducted in the range of  $V_{rn} = 4$  to 10.

Previous studies show considerable sensitivity of VIM amplitudes to current heading [1, 3, 4, 6, and 7]. Therefore, tests are done in increments of 10 degrees. For the present tests, both the strakes and anode pattern repeats every 120 degrees. The chains and pipes do add some asymmetry to that pattern. Hence, in order to optimize test time, for the tests without chains and pipes, tests are only done in the range 0 to 120 degrees. The range of headings is expanded for the tests with chains and pipes.

## MODEL TESTS

### Spar model parameters

The diameter of the model spar is 5.74 ft. (1.75m), which at a scale of 1:22.3 corresponds to a prototype diameter of 128 ft. (39m), a typical size for Gulf of Mexico (GoM) spars. The draft is 9.68 ft. (2.95m), corresponding to a prototype draft of 216 ft. (65.8m), typical of GoM truss spars.

The spar hull is outfitted with chains, pipes, and anodes typical of spar designs today. A plan view of the model is shown in Figure 1. The strakes are a typical 3-start design, with a strake height equal to 13% of the hull diameter (typical for some GoM spars) and a pitch of 4:1, which falls in the range of spars in the field today. A layout view of the appurtenances on the model is shown in Figure 2.

The spar model is centered under the carriage and connected to the carriage through four lines at 45 degrees. These lines are made of three segments; a cable, a spring and another cable. To achieve isotropic stiffness, the lines are arranged at 45 degrees, so the encompassing box is square. See Figure 3.

The springs are an intrinsic part of the system. The global stiffness is chosen such that the tests have a Reynolds Number of approximately  $10^6$  at a  $V_{rn}$  of 6 and a Froude Number of approximately 0.25 at a  $V_{rn}$  of 10. The first requirement is to enforce a super-critical regime, the latter to minimize the bow wave heights at the fastest tow speeds.

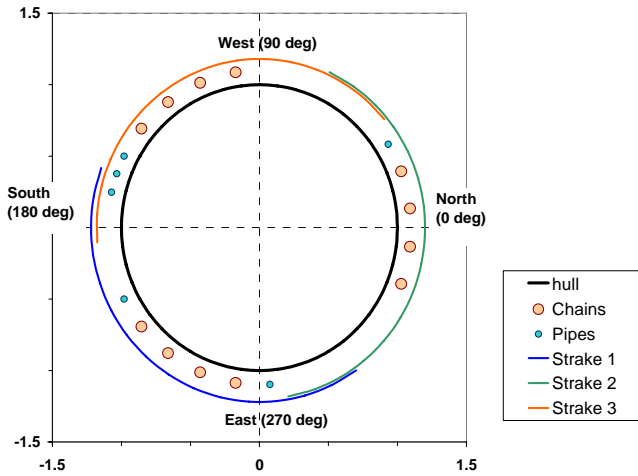


Figure 1: Plan view of spar appurtenances

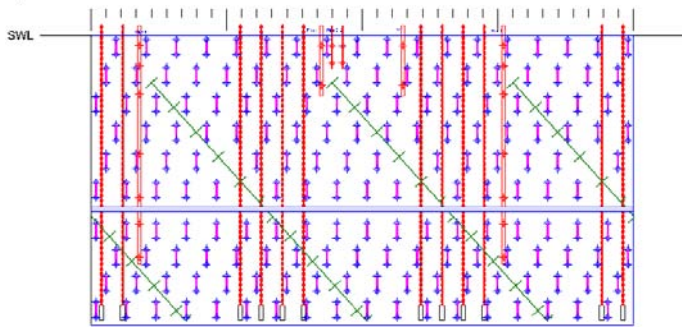


Figure 2: Layout view of spar appurtenances

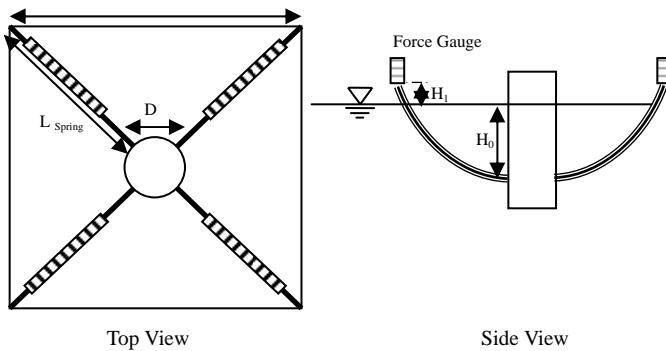


Figure 3: Schematic of spring system for model tests

Figures 4 - 7 shows the model from the four cardinal angles.

Fig. 4: Base Case: All appurtenances are on the hull. They include chains, pipes, anodes and strakes.

Fig. 5: Variation 1 - Chains and pipes removed. Model includes strakes, anodes and fairleads

Fig. 6: Variation 2 - Hull is bare, except for the strakes.

Fig. 7: Variation 3 - Hull is complete except for anodes.



Figure 4 – Base Case

Figure 5 – Variation 1



Figure 6 – Variation 2

Figure 7 – Variation 3

Figure 8 shows a close-up of the appurtenances looking down on the base case configuration model.

Heading changes are performed after each run. In order to rotate the model but keep the spring and the force gauges fixed under the carriage, a rotating ring is built into the model. That ring (shown in Figure 9) connected the spring system to the model, which could rotate freely inside it when loose. When tightened the model was fixed at the chosen heading. Four struts are placed at increments of 90 degrees. These struts allow for clearance of the spring connection through the strakes, hence a minimal gap in the strake is necessary.

### System Identification Tests

A GM test is performed to ensure model stability, and to ensure dynamic similitude to the low Reynolds Number model tests (not discussed in this paper). In order to avoid coupling between angular and lateral motions, the sway to pitch ratio is kept greater than 3. Therefore, the effect of the GM on the pitch and roll motion is not significant.



Figure 8: Detailed view of appurtenances, base case model

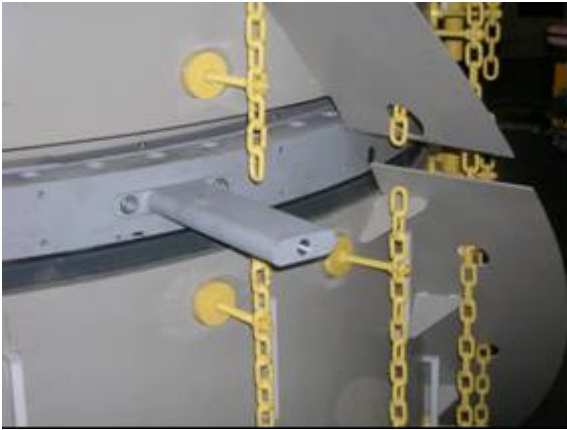


Figure 9: Ring rotation system for model

The roll and pitch period is calculated from:

$$T_{Roll} = 2\pi R_x \sqrt{\frac{1 + \mu_{55}/M}{gGM}} \quad (3)$$

where  $R_x$  is the radius of gyration around the  $x$ -axis,  $\mu_{55}$  the roll added mass,  $M$  the mass and  $GM$  the metacentric height.

Decay tests are performed for lateral and angular motions to measure the natural frequency of the system. Because of the symmetry of the system, pitch and roll have the same natural frequencies, and surge and sway have the same natural frequencies. The system damping is also obtained from the decay tests, assuming the motion is governed by:

$$(M + \mu)\ddot{x} + B\dot{x} + Kx \quad (4)$$

Where  $x$  is the displacement,  $\dot{x}$  the velocity,  $\ddot{x}$  the acceleration,  $\mu$  the added mass,  $B$  the damping and  $K$  the stiffness of the system.

The critical damping,  $C_o$ , and undamped natural frequency,  $\omega_0$ , are:

$$C_o = 2\sqrt{K(M + \mu)} \quad (5)$$

$$\omega_0 = \sqrt{\frac{K}{M + \mu}} \quad (6)$$

And the damping ratio is

$$\zeta = \frac{B}{C_o} \quad (7)$$

The dynamic properties from these tests are found in Table 1.

Table 1: Dynamic properties of the model

$M$	Mass = displaced Volume $\times \rho$	7088 kg
$M+\mu$	Mass + added mass = 2 x M	14176 kg
$B$	Damping	2.8 Kg/s
$K$	Global Stiffness	2111 N/m
$C_o$	Critical Damping	255 Kg/s
$\zeta$	<b>Damping ratio</b>	<b>1.10%</b>

Static offset tests are performed by pulling on the model and measuring the force necessary to hold the model in place at a prescribed offset. In these tests, they are used to check the stiffness of the global system. Prior to rigging the model, the individual spring stiffnesses are checked by hanging the spring vertically, attaching a known weight to the end and measuring the elongation in the spring. (7)

Drag tests are performed to measure the base drag coefficient of the cylinder when not undergoing VIM oscillations. To constrain the cylinder, the upstream springs are bypassed by a steel cable. Stiff springs are connected between the force gauges and the lines to protect the gauges during the deceleration phase.

The spring load cells are mounted at their carriage connection points rather than on the model. Since the springs required to resist the motion of the model at such large scale were fairly robust and large, they have a larger relative projected area than similar tests of smaller scale. Therefore, drag tests are performed without the cylinder to measure the drag coefficient from the springs alone. The spring Cd is subtracted from the drag tests. Results for the base case model are shown in Figure 10 for both the springs and for the base case model with spring Cd removed.

One of the purposes of the baseline drag tests is to help determine whether or not there is a significant Reynolds Number effect on the drag coefficient. To that end, tow tests are done at velocities well below the speeds required to meet the target reduced velocities for the VIM test program. The tow tests span the range represented by the drag bucket for a smooth circular cylinder [8]. As shown in Figure 11, there is only a modest change in drag coefficient over the Range of  $Re = 190,000$  to  $1,750,000$  with no definite trend observed.

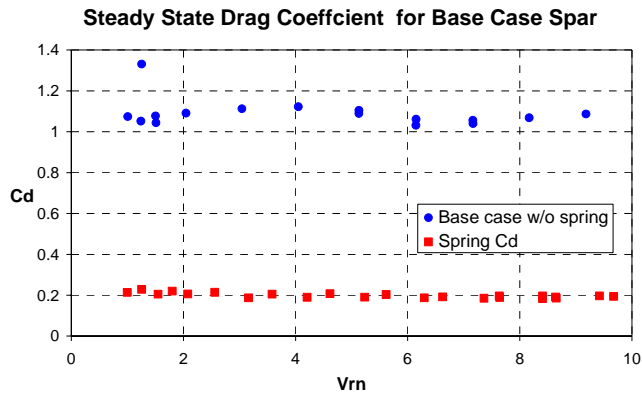


Figure 10: Drag for Base Case Model and Springs

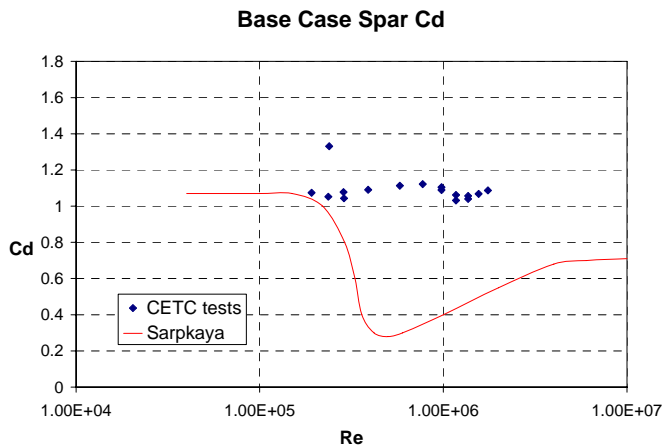


Figure 11: Drag Coefficient for Base Case Model vs. Re.

### Test Program

The four configurations used in the test program are all done with the same hull model to minimize costs. Initially, all appurtenances (strakes, chains, pipes, anodes) are attached to the model. This is the “base case” model. Static offset tests are done on this model to check the stiffness of the global system. Prior to rigging the model, the individual stiffness of the spring is checked by hanging the spring vertically, attaching a known weight to the end and measuring the elongation in the spring. Decay tests are performed to measure the natural frequency of the system. The tests are performed for lateral and angular motions. Because of the symmetry of the system, both pitch and roll and surge and sway respectively have the same natural frequencies.

Ninety two (92) tests are done with the base case model, as summarized in Table 2. In order to optimize tank time, the model is towed in both directions. For some cases, the same test is repeated in both directions to confirm there are no tow direction dependencies in the results.

The model heading is changed while the tank is settling down from the previous run. An ingenious system developed by the DTMB engineers facilitates the changes in model heading, but it is still quite tedious to rotate such a massive model. Nevertheless, the change in heading is often completed by the time the basin has calmed down from the previous run.

Twenty two headings are tested with the base case model for reduced velocities ranging from 4 to 10. Due to the high loads on the spring system, only the tests with the lowest VIM amplitudes are tested out to  $Vrn = 10$ , with other headings tested up to  $Vrn$  of 9 to 9.5. The Froude Number and Reynolds Number associated with each reduced velocity are given in Table 3.

The next configuration tested, with chains and pipes removed, is referred to as Variation 1. Sixteen headings from 0 to 150 degrees are tested, at reduced velocities ranging from 4 to 9.

Next, the anodes are removed from the model. This configuration (strakes only) is referred to as Variation 2. Since the application of the anodes is a fairly time consuming process, this configuration is tested after Variation 1. Just as with Variation 1, system properties are determined by decay tests. Only 13 headings are tested with this configuration (0 to 120 deg.), with reduced velocities ranging from 4 to 9.

Finally, chains and pipes are added back to the model. Decay tests are done with this final configuration (Variation 3). A total of 19 headings are tested, with  $Vrn$  ranging from 4 to 9.

Table 2: Test Matrix Summary

Configuration	Headings Tested	No. of Runs
Base Case	-30 to 170 deg.	92
Variation 1	0 to 120 deg.	43
Variation 2	0 to 120 deg.	36
Variation 3	-30 to 150 deg.	69
<b>Total No. of Runs</b>		<b>240</b>

Table 3: Summary of Froude and Reynolds Numbers

$Vrn$	$Fr$	$Re$
4	0.109	6.99E+05
5	0.136	8.73E+05
6	0.163	1.05E+06
7	0.191	1.22E+06
8	0.218	1.40E+06
9	0.245	1.57E+06
10	0.272	1.75E+06

## RESULTS

Numerous response quantities are analyzed from the test program: drag and lift loads (essentially, system damping), 6 DOF motion response and statistics, observed response periods, number or response cycles to name a few. The focus of this paper is only the maximum transverse VIM. This value is reported as response amplitude divided by diameter, or A/D. The maximum A/D is defined as  $(A_{max} - A_{min})/2D$  where  $A_{max}$  is the maximum sway displacement and  $A_{min}$  the minimum sway displacement measured during the entire test.

Record length is a concern for tow tests due to the limited length of model basin, even with the longest tanks in the world. The number of cycles kept for statistical analysis (after removal of start-up transients) varied from a low of 15 for the highest reduced velocity (10) to 35 cycles for the lowest reduced velocity (4). Previous work [7] shows that the statistics for repeat runs are comparable to those from a very long record. Based on that earlier work, repeat runs are done for critical tests. In order to incorporate the benefit of multiple similar runs, a Weibull distribution is fitted to the right tail (largest) of the extreme values by minimizing the least squares relative error over approximately the largest 20% of the ordered statistics.

From the Weibull fit, a 1-hour full-scale time level or return period is chosen with the concatenation of runs characterized by the corresponding fitted A/D. Examples of fitting a Weibull distribution to 1 run and 5 runs are shown in Figures 12 and 13. In this example, the base case data was used with  $V_{rn} = 7$  and heading = 0 degrees. In this example, the Weibull fit was extrapolated to produce an estimated 1 hour maximum value of 0.51 for the single run, and interpolated to produce an estimated maximum of 0.45 for the 5 concatenated runs.

Various combinations are tried and the fitted maximum A/D values are shown as a function of number of runs in Figure 14. The accuracy increases with the number of repeat runs, and stabilizes at around 4 to 5 repeats.

It is not possible to present all of the results from all of the configurations, headings, and tow speeds from the present test program. However, indicative time series results are presented below for 3 reduced velocities from the base configuration.

Figure 15 shows the surge/sway trajectory and time series for a run on the “lock-in” slope (reduced velocities above the threshold but below lock-in values). In this range, the response is highly modulated, and tends to lock in and out of VIM several times.

Figure 16 shows the same quantities for a reduced velocity of 7 at a heading which is essentially “locked-in” to VIM; and Figure 17 shows the same quantities just beyond the locked-in range, at a reduced velocity of 8.5, and exhibits more modulation in the signal than that at lock-in. Eventually, as the

reduced velocity gets larger, the response should lock-out. However, it is not possible to test to lock-out conditions with the present set-up.

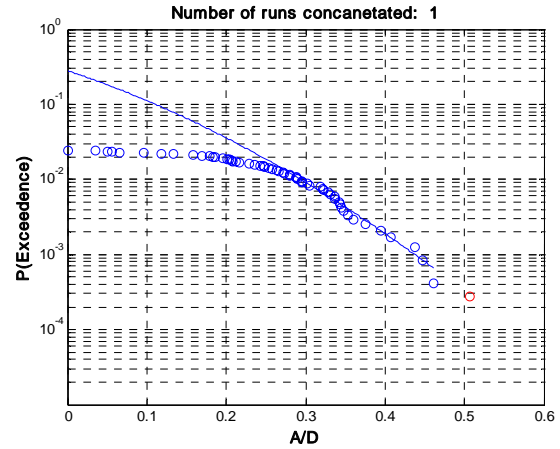


Figure 12: Weibull fit to a single run

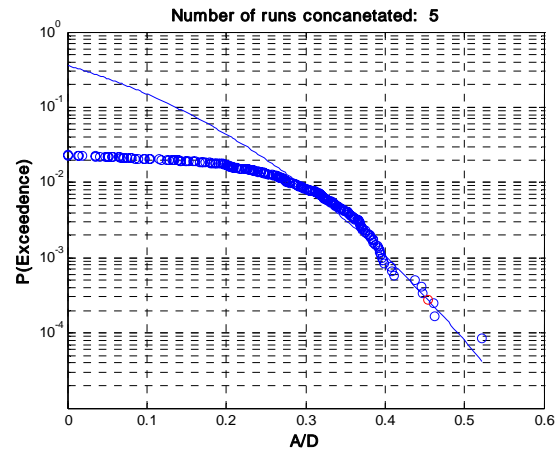


Figure 13: Weibull fit to 5 concatenated runs

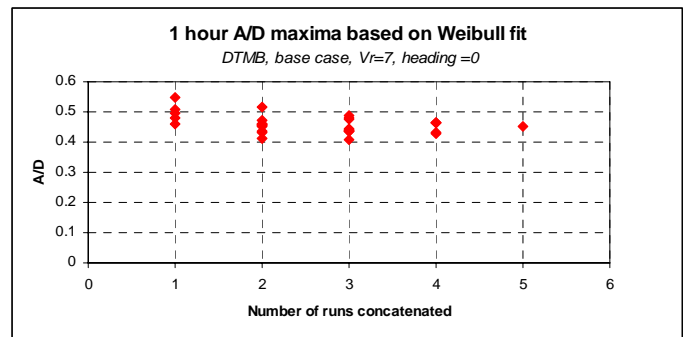


Figure 14: Fitted A/D vs. Number of Runs

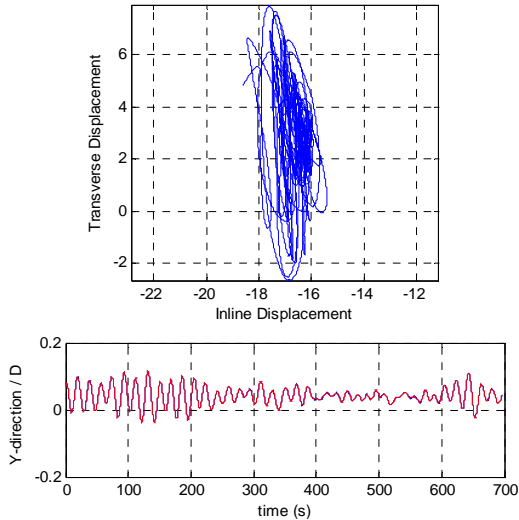


Figure 15: Trajectory and Time History for Sample Vrn=5

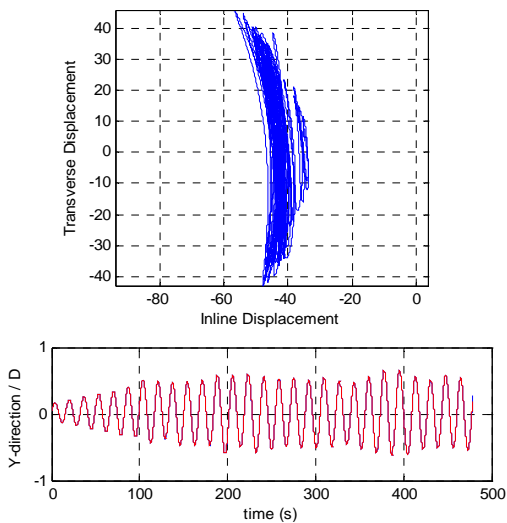


Figure 16: Trajectory and Time History for Sample Vrn=7

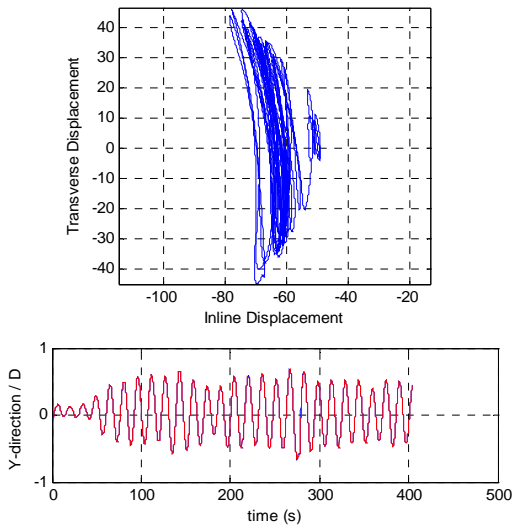


Figure 17: Trajectory and Time History for Vrn=8.5

Figure 18 shows a sample plot of max A/D vs. Vrn for the base case model, for the 30 degree heading. This plots shows how the A/D increases from a threshold value near 0 at a reduced velocity of 4, up to a maximum value “locked-in” at a reduced velocity of 8, before slightly tapering off up to a reduced velocity of 9.

Figure 19 shows the results for the same model at a heading of 90 degrees. The strakes are more effective for this heading, but the same trend of increasing response above a reduced velocity of 4 and tapering off at some peak Vrn value (in this case, the peak occurs at a Vrn of 7), before tapering off up to a Vrn of 10 is observed.

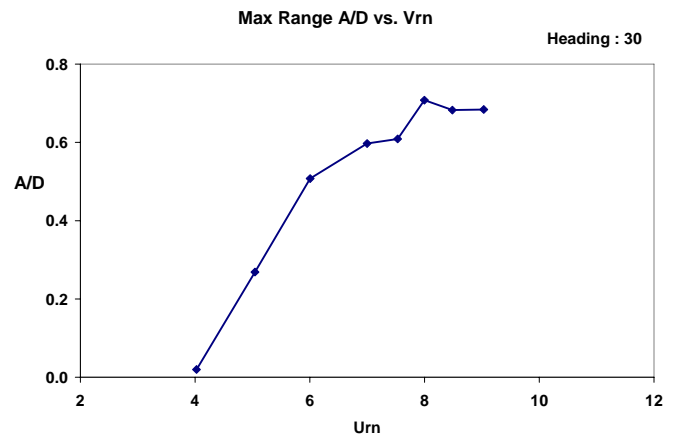


Figure 18: Variation of max A/D vs. Vrn, 30 degrees

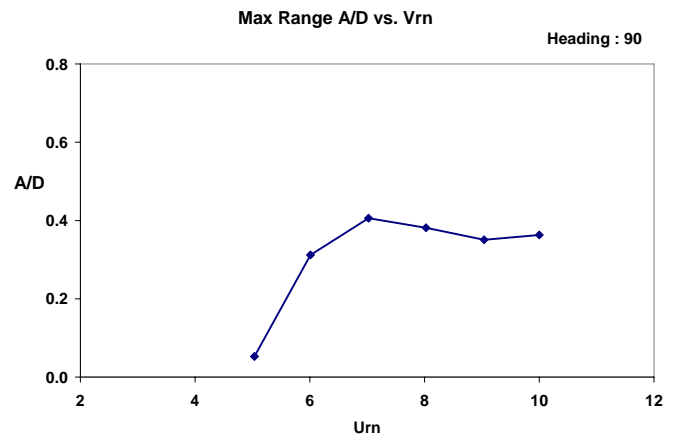


Figure 19: Variation of max A/D vs. Vrn, 90 degrees

One of the more intriguing results in these tests is shown in Figure 20: the comparison of the base case VIM response vs. heading against the bare cylinder with strakes at a reduced velocity of 7.

In this case, it appears that the strakes on the bare model perform reasonably well over all headings. Between the headings of 20 and 70 degrees, there is virtually no response.

At headings near 0 and between 90 and 120 degrees, there is some response, but at modest amplitudes. However, when there are chains, pipes, and anodes present, the response is actually greatest where the strakes worked the best for the bare model!

This one plot highlights how critical it is to accurately model the geometry of the spar when developing design criteria for the spar. It is the basis of the advice from those who do model tests to those who design spars: “build what you test, and test what you build.”

Similar data is plotted in Figure 21 in a polar plot. However, instead of comparing the base case against the bare cylinder model, the base case is compared to the model with anodes and strakes only. In this plot, the heading represents the angle at the leading edge of the spar during testing, or conversely, the heading from which a current would be approaching the spar.

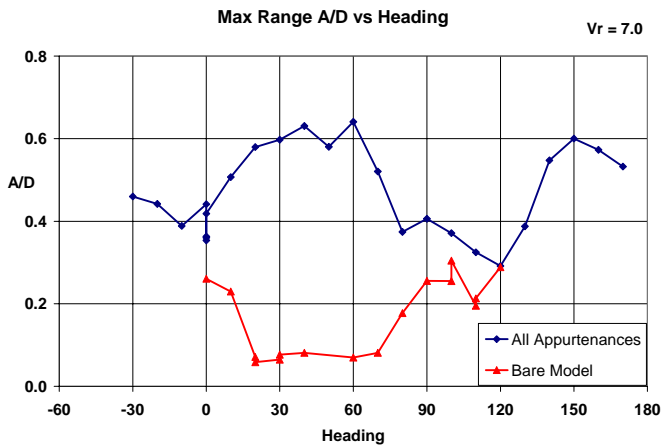


Figure 20: A/D Comparison Between Base and Bare Case with strakes

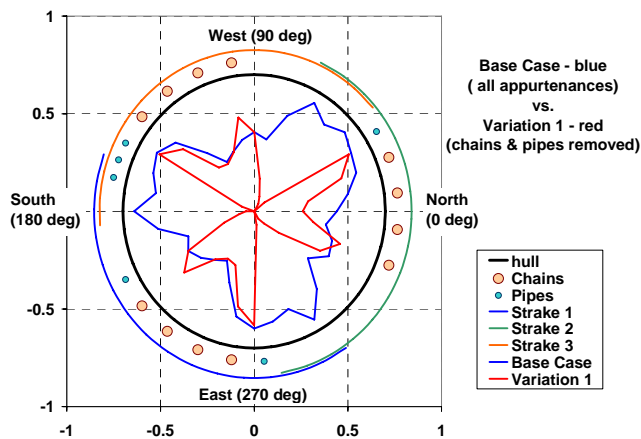


Figure 21: Polar Plot of A/D for Base and Bare Case

This plot more clearly shows the distinct effect of the chains and pipes, since that is the only difference between the two models.

## CONCLUSIONS

The primary purposes of these tests are to

- Demonstrate the capability to perform super-critical Re tests for offshore structures such as a truss spar hull,
- Develop a set of data that could be used to validate numerical tools (see [9] for an example application),
- Compare results against identical model tests at smaller scales, and
- Develop VIM model test guidelines regarding test methodology, model geometry, and model scale

All objectives of the test program are accomplished. This paper only focuses on the super-critical Re tests. We have found that it is possible to model the effect of appurtenances such as chains and anodes on the VIM response and strake effectiveness under super-critical conditions without resorting to complicated actuator rigs and similar systems, and without being restricted to 1- and 2-DOF models. We have also shown that chains and pipes have a major impact on the effectiveness of strakes. Further, the data developed in these tests are being used to validate CFD models [9]. And finally, we have the data now to complete a comprehensive review of the importance of Reynolds Number in VIM testing. The evaluation against the sub-critical Reynolds Number tests is beyond the scope of this present paper.

## ACKNOWLEDGMENTS

The authors would like to thank Chevron for funding the majority of these tests, and allowing the publication of the results. They would also like to thank Leif Smitt from Force Technology, who helped with the design of the test rig and model properties development, and the staff at DTMB, who did such a great job completed this work on time under a very tight budget, in particular Dave Coakley and Kevin Kimmel. Finally, we would like to thank our partner Shell, and their representative, Stergios Liapis, who participated during the model test portion of the program.

## GLOSSARY

- A/D Non dimensional number (Amplitude over Diameter), a measure of VIM lateral excursion
- B Damping of a system
- $C_0$  Critical damping
- $C_d$  Drag Coefficient
- $C_l$  Lift Coefficient
- $Fr$  Froude Number, ratio of inertia over gravity terms
- GM Metacentric height, a measure of stability influencing the angular frequency response.

K	Stiffness of a system
M	Mass of a system
R <sub>xx</sub>	Radii of Gyration in roll
Re	Reynolds Number, ratio of Inertia versus viscous terms
T	Natural period
T <sub>n</sub>	Natural period in calm water
VIM	Vortex Induced Motions, as applied to spar type offshore platforms
VIV	Vortex Induced Vibration, as applied to risers with multiple modal responses
V <sub>rn</sub>	Reduced velocity based on natural frequency in quiescent conditions
$x$	Displacement
$\dot{x}$	Velocity
$\ddot{x}$	Acceleration
$\lambda$	Scale factor, as defined by the significant length of prototype / model
$\mu$	Added mass
$\zeta$	Damping ratio.

## REFERENCES

- [1] Spar Vortex Induced Motions, Workshop sponsored by OTRC and US-DOI Minerals Management Service, October 22-24, 2003, Camp Allen, Texas.
- [2] Sarpkaya, T. and Isaacson, M., "Mechanics of Wave Forces on Offshore Structures", Van Nostrand Reinhold Company, New York, 1981.
- [3] Sandström, R. E., Yung, T-W., Slocum, S. T. and Ding, Z. J., "Advances in Prediction of VIV for Spar Hulls", Deep Offshore Technology Conference, Marseille, France, 19-21 Nov 2003.
- [4] Yung, T. W., Sandström, R. E., Slocum, S. T., Ding, J. Z. and Lokken, R. T., "Advancement of Spar VIV Prediction", OTC 16343, 2004.
- [5] Cowdrey, C. F. and Lawes, J. A. "Drag Measurements at High Reynolds Numbers of a Circular Cylinder Fitted with Three Helical Strakes", NPL/Aero/384, National Physical Laboratory (UK), July, 1959.
- [6] Finn, L.D., Maher, J.V., and Gupta, H., "The Cell Spar and Vortex Induced Vibrations," OTC 15244, 2003.
- [7] Finnigan, T, Irani, M, and van Dijk, R, "Truss Spar VIM in Waves and Currents", OMAE 2005-67054., Greece, 2005
- [8] Sarpkaya, T. "Inline and Transverse Forces on Cylinders in Oscillatory Flow with High Reynolds Numbers" Journal of Ship Research, 21, 200-216, 1977
- [9] Oakley, Jr., O.H. & Y. Constantinides, 2007, "CFD Truss Spar Hull Benchmarking Study", Proc. of the 26th Int. OMAE Conf., OMAE2007-29150.